EUROFUSION WPMAT-PR(16) 16149

A Sand et al.

Cascade fragmentation: impact on primary radiation damage

Preprint of Paper to be submitted for publication in
Materials Research Letters

This work has been carried out within the framework of the EUROfusion Consortium and has received funding from the Euratom research and training programme 2014-2018 under grant agreement No 633053. The views and opinions expressed herein do not necessarily reflect those of the European Commission.

Analytical size-frequency distributions of vacancy and self-interstitial defects in neutron irradiated tungsten

A. E. Sand,[1, a)] A. De Backer,[2] K. Nordlund,[1] and S. L. Dudarev[2]
[1)] *Department of Physics, P. O. Box 43, FI-00014 University of Helsinki, Finland*
[2)] *CCFE, Culham Science Centre, Abingdon, Oxon OX14 3DB, UK*

(Dated: 15 June 2016)

The size of defect clusters, produced athermally by energetic recoils under ion or neutron irradiation, has a strong impact on the subsequent thermal evolution of microstructure, and hence on the radiation response of materials. We develop a model to describe the size distribution of vacancy and self-interstitial defect clusters in neutron irradiated tungsten, based on the statistics of subcascade splitting in energetic collision cascades, and the distribution of primary defects formed in individual sub-cascades. This model of defect production is valid for all defect sizes, with a well-defined upper size limit, agrees with experiments, and as such can be used for generating the initial conditions for simulations of microstructural evolution.

The athermal formation of defect clusters occurring as a direct result of collision cascades induced in a material by incident neutrons or energetic ions drives microstructural evolution of the material under irradiation. This is especially true in tungsten (W), where the large atomic mass and high subcascade splitting energy threshold leads to dense cascades[1] and the formation of large defects readily visible in an electron microscope[2]. It has recently been determined, both by molecular dynamics (MD) simulations[3] and transmission electron microscopy (TEM) observations[2], that the distribution of defects as a function of their size has a power-law form

$$f(N) = \frac{A}{N^S} \tag{1}$$

where N is the size of defect clusters, and S is a scaling size exponent. A is a pre-factor that is proportional to the experimental or simulated defect cluster production rate. The above scaling law, with $S \approx 1.63$ for self-interstitial clusters in W, is strikingly similar to the scaling law describing the fragmentation of spherical gypsum balls discovered by Oddershede *et al.*[4]. Their study showed that the slope of the scaling law depended on the shape of the fragmenting piece, rather than the material, with a slope of $S = 1.63$ found for spherical pieces. In simulations of collision cascades in W, the larger defects are mainly formed in the most spherical region of cascades[1], and hence spherical cascade geometry dominates also the formation of larger defects in the primary damage in W.

However, the tail of the distribution cannot be deduced from MD simulations alone, due to the rare occurrence of very large clusters. The better statistics provided by ion irradiation experiments[2] reveal a sharp increase in the slope of the distribution for defect sizes above those observed in simulations.

In this Letter we develop a model to explain the deviation from the simple power law behaviour in Eq. 1. We base the model on the formation of subcascades, since the cascade-induced formation of large defect clusters in metals occurs in the dense heat spike regions, due to the dynamics of the recrystallization front in the heat spike[5–9]. Hence the formation of such defects depends sensitively on subcascade splitting. It is well known that low-energy (with energies from 1 to 10 keV) recoils in heavy metals produce damage in nearly spherical heat spikes[5,7]. With increasing recoil energy, the cascades start splitting up into spatially separated subcascades[10,11]. This is not a sharp transition: even above the "subcascade breakdown energy", some cascades remain "compact", i.e. form a single roughly spherical collision region[12]. Conversely, below the threshold energy, subcascades may exhibit partial splitting. This is because the nuclear collision cross section gradually decreases as a function of energy, leading to atomic recoils travelling increasing distances between collisions[13].

Figure 1 illustrates the development of a heat spike and subsequent defect formation. At the peak of the heat spike damage, the disordered cascade core is surrounded by an expanding pressure wave which deforms the material far outside the liquid core. The large defect clusters remaining after 15 ps form in the disordered core region. Hence the disordered, or "liquid", volume of subcascades defines a natural upper bound on the size of defects that can form athermally.

Size-frequency distributions of defects derived from MD simulations of cascades in W for various primary knock-on atom (PKA) energies are shown in Fig. 2. Despite the limited statistics for 100 and 200 keV cascades, it is clear that the same scaling law applies at all energies, with the overall frequency proportional to the cascade energy. Single defects and clusters containing only a few ($N = 2 - 3$) defects also follow power laws, but with a slope steeper than that exhibited by larger defects, for both vacancies and self-interstitial atoms (SIAs).

In cascades where subcascade splitting occurs, the probability of forming a large defect is subject to the probability of occurrence of subcascade pockets which are large enough to contain the defect. To find the largest possible defect size from a given subcascade, we use the

[a)] Corresponding author andrea.sand@helsinki.fi

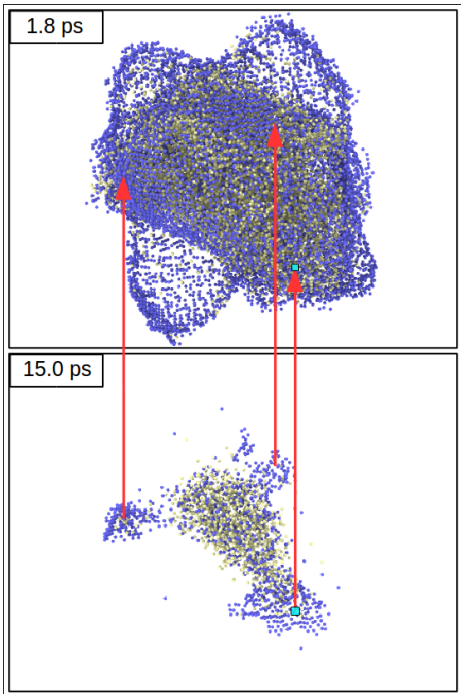

FIG. 1: (Color online) Top: a snapshot of a 150 keV cascade in W at the maximum extent of the heat spike at 1.8 ps. Below: defects form as the cascade cools and the lattice recrystallizes. Final positions of the defects are indicated relative to the maximum extent of cascade damage. Blue (yellow) spheres represent interstitials (vacancies). Details of the simulation are given in Ref.[3].

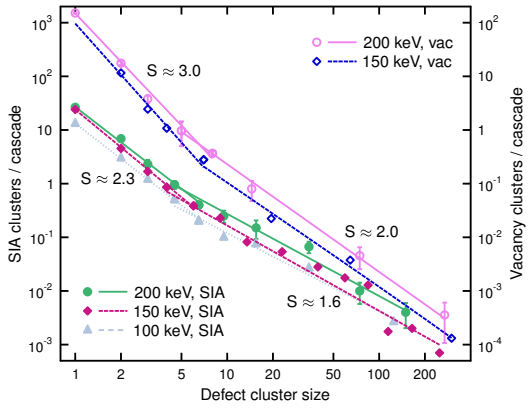

FIG. 2: Size-frequency distributions of defects in W derived from MD simulations of cascades initiated by PKAs with various energies. Note the different slopes of scaling laws for SIAs and vacancies. For clarity the vacancy plot is shifted upwards with respect to the SIA plot. The scale of the axes remains the same.

spherical liquid volume approximation. Noting the fact that interstitial clusters in W form 2-dimensional dislocation loops, and assuming the loops have the $1/2\langle 111\rangle$ Burgers vector, we arrive at the maximum possible size N_D^{int} of an interstitial-type defect as a function of the diameter D of the liquid region as[2]

$$N_D^{int} \approx \pi\sqrt{3}(D/(2a_0))^2, \tag{2}$$

where $a_0 = 3.165$ Å is the lattice parameter of W.

The formation of vacancy clusters is inherently different from that of SIA clusters, for example the exponents of scaling laws in Fig. 2 are different for vacancies and SIAs. The liquid core of the cascade contains almost all the vacancies, which are pushed towards the center by the recrystallization front. In most cases, a single (often diffuse) vacancy cluster is formed in the center of a spherical cascade volume, usually surrounded by a cloud of single vacancies. Multiple vacancy clusters form only if the liquid core is split into several domains, either in space or time. In the events where clustering is especially effective, almost all the vacancies condense into one large cluster.

By the law of mass conservation, the largest conceivable vacancy cluster thus contains the same number of point defects as the total number of SIAs produced in the cascade. We expect that, at most, an area corresponding to twice the projected area of the spherical cascade core or, equivalently, half of the surface area, contains the SIA clusters. In addition, we disregard the relatively small numbers of isolated crowdions formed far from the heat spike as a result of replacement collision sequences. Hence we can relate the diameter D of the liquid region to the largest possible vacancy cluster N_D^{vac} given by

$$N_D^{vac} \approx 2\pi\sqrt{3}(D/(2a_0))^2. \tag{3}$$

We point out that this formula does not assume any specific geometry for the vacancy cluster, and is valid irrespective of whether the final cluster is a 3-dimensional depleted zone[14], or a dislocation loop.

To find the total frequency $f(N_D)$ of a cluster of size N_D, we are interested in the *frequency of occurrence of subcascades which are larger than the limiting size* D. The fractal nature of cascades[15] leads us naturally to look for a power law distribution of subcascade sizes, which in the upper size limit reaches a critical point N_c, where all the cascade energy is contained in a single compact cascade. This suggests introducing a "critical" exponent κ combined with a "reduced size" of the subcascade $n = (N_c - N)/N_c$. We thus expect the probability of formation of a subcascade large enough to accommodate a defect of size N to be given by

$$f_{SC}(N) = B((N_c - N)/N_c)^{\kappa}, \tag{4}$$

where B is the average total number of subcascades. In the limit of small N, every subcascade is large enough, and accordingly $\lim_{N\to 0} f_{SC} = B$.

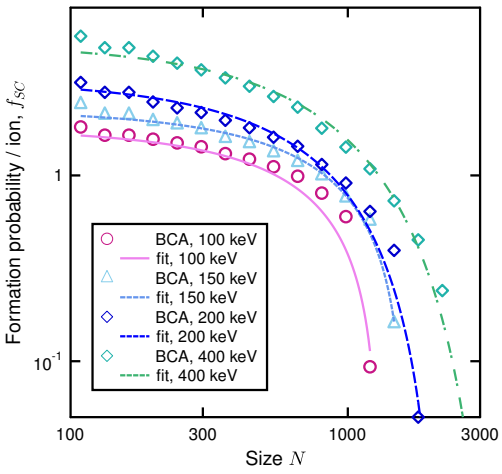

FIG. 3: Fit of Eq. 4 to the BCA prediction of the probability of formation of subcascades large enough to contain a defect of size N (see text for details).

The frequency of occurrence of a defect of size N in a single cascade volume can now be weighed by the frequency of occurrence per ion of a subcascade of sufficient size, giving the total size-frequency distribution of defects as

$$f(N) = \frac{A}{N^S} \times B((N_c - N)/N_c)^\kappa. \qquad (5)$$

Here we choose not to make any generalizing assumptions, but rather consider the parameters as PKA energy dependent, and determine them by fitting to the simulation data. We find parameters for the distribution of subcascade sizes (Eq. 4) using a recently developed method, detailed elsewhere[17], based on the binary collision approximation (BCA)[18]. We have simulated 200 cascades with the BCA method for each PKA energy. The frequency of occurrence of subcascades larger than N predicted by these calculations is shown in Fig 4, and follows very closely the distribution in Eq. 4.

The BCA subcascade distributions are the same for SIA and vacancy clusters, with only the N_c parameter changing due to the different mechanisms of cluster formation, leading to different maximum cluster sizes. The final distributions are different for vacancies and SIAs due to the different scaling laws derived from MD simulations (Fig. 2). To find the final distributions, we assume that the MD results are accurate in the defect size range that they cover, which do not include the tail in the limit of large defect sizes. Furthermore, we recognize that partial subcascade splitting already affects the distributions derived from MD at these PKA energies. We therefore fit the parameters S and A in the full distribution function

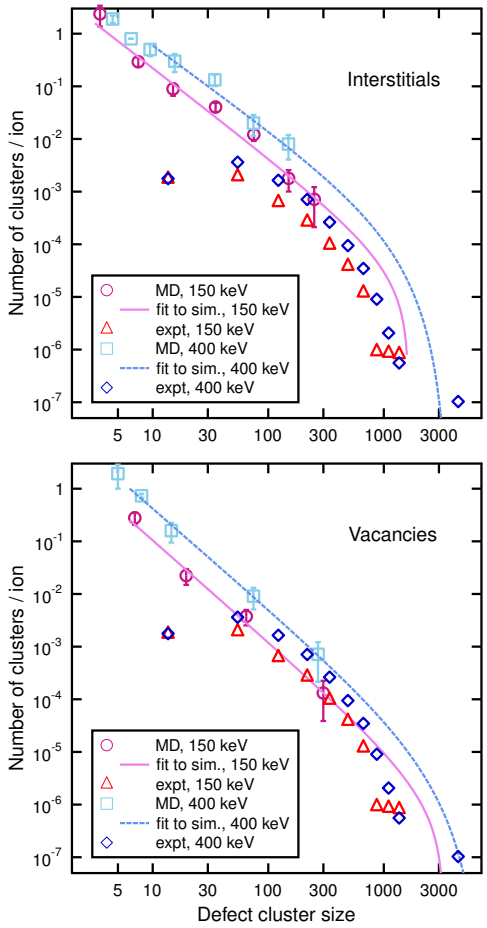

FIG. 4: Comparison of model for SIA (top) and vacancy (bottom) cluster size distributions against experimental data[2]. MD distributions for 400 keV were obtained by scaling the 200 keV data by a factor of 2.

Eq. 5 directly to the MD results, with parameters B, N_c and κ determined by the fit to the BCA subcascade distribution. To allow comparison with experiments performed using 400 keV ions[2], we recall that the frequency of defects in MD simulations is proportional to the PKA energy (Fig. 2), and thus multiply the frequency in 200 keV cascades by 2, to obtain the distribution for the 400 keV cascades. The final parameters for the best fit are given in Table I.

In bulk cascades, the total numbers of vacancies and SIAs should be equal, despite the different statistics. As a consistency check, we calculate the total number of defects N_{tot} of each type, by integrating $Nf(N)dN$ over the full range of the distributions, where $f(N)$ is given by Eq. 5. Since point defects and small clusters in the range $N \sim 2-3$ follow different scaling laws, we integrate over $4 \leq N \leq N_c$, and use the clustered fraction

TABLE I: Parameters for the size-distribution from fits to BCA and MD data, the clustered fraction of defects F_{Cl} determined from MD, and the total number of point defects N_{tot} predicted by the model. The parameters B, N_c and κ were determined from the BCA data alone, after which A and S were determined by fitting the complete model in Eq. 5 to the MD data. The error bars are statistical uncertainties obtained using the Levenberg-Marquardt least squares fitting algorithm[16]. Fitting was performed assuming a 10 % statistical uncertainty on all data points.

Interstitials							
Energy (keV)	A	S	B	N_c	κ	F_{Cl}^{SIA}	N_{tot}^{SIA}
150	4.94 ± 0.52	1.70 ± 0.03	2.26 ± 0.12	1642 ± 60	1.17 ± 0.16	0.75 ± 0.05	270 ± 20
200	3.65 ± 0.27	1.62 ± 0.03	3.26 ± 0.11	2200 ± 1	2.36 ± 0.06	0.8 ± 0.1	360 ±
400	4.65 ± 0.34	1.62 ± 0.03	5.14 ± 0.22	3687 ± 191	3.79 ± 0.39	0.8 ± 0.1	820 ±
Vacancies							
Energy (keV)	A	S	B	N_c	κ	F_{Cl}^{vac}	N_{tot}^{vac}
150	3.94 ± 0.60	1.93 ± 0.04	2.26 ± 0.11	3284 ± 120	1.17 ± 0.16	0.2 ± 0.1	340 ± 100
200	5.21 ± 0.61	1.91 ± 0.03	3.26 ± 0.11	4400 ± 2	2.36 ± 0.06	0.35 ± 0.05	385 ±
400	6.64 ± 0.78	1.91 ± 0.03	5.14 ± 0.22	7374 ± 382	3.79 ± 0.39	0.35 ± 0.05	790 ±

of defects F_{Cl} derived from MD simulations to determine N_{tot}. The results are given in Table I. Good agreement is found between the predictions for SIAs and vacancies, although a relatively large uncertainty in the fraction of clustered vacancies in 150 keV cascades gives rise to a large uncertainty in the total vacancy count.

Figure 4 compares our model with experimental data from recent TEM observations of self-ion irradiated W[2]. The vacancy cluster data are compared assuming a 2-dimensional dislocation loop configuration for the vacancy clusters, which is expected to result from cascade collapse[19], a phenomenon that MD simulations reproduce relatively rarely[1,20]. Our results show agreement between distributions of defects of both types with TEM observations, but the frequency of SIA loops predicted by MD is much higher than the frequency of occurrence of loops visible in the micrographs. Possible reasons for this overprediction are a) TEM observations have not been corrected for the loop loss to the surface, b) diffraction conditions render loops with a certain orientation invisible, and c) the presence of a surface in ion irradiation of foils reduces the frequency of large interstitial defects due to interstitial loop glide to the surface[21], which is not accounted for in the MD results. On the other hand, the simulated frequency of vacancy clusters agrees well with experimental frequency, except in the large size limit. This may indicate that diffuse clusters and voids tend to collapse into loops in the mid size range, while the largest vacancy clusters tend to remain voids.

In conclusion, we have presented a model for the distributions of SIA and vacancy type defects produced from energetic cascades in irradiated W. The distributions are different for different defect types, due to their different formation mechanisms. In addition, the effective power law exponents seem to change in the limit of very small clusters. The model provides well defined upper limits to the distributions, which in turn can be used as input for microstructural evolution models.

This work has been carried out within the framework of the EUROfusion Consortium and has received funding from the Euratom research and training programme 2014-2018 under grant agreement No 633053, and was part-funded by the RCUK Energy Programme [grant number EP/I501045]. The work was also supported by the Enabling Research project TriCEM on Tritium Retention in Controlled and Evolving Microstructure. Grants for computer time from the Center for Scientific Computing in Espoo, Finland, are gratefully acknowledged. The views and opinions expressed herein do not necessarily reflect those of the European Commission.

[1] A. Sand, K. Nordlund, and S. Dudarev, J. Nucl. Mater. **455**, 207 – 211 (2014).
[2] X. Yi, A. E. Sand, D. R. Mason, M. A. Kirk, S. G. Roberts, K. Nordlund, and S. L. Dudarev, EPL **110**, 36001 (2015).
[3] A. E. Sand, S. L. Dudarev, and K. Nordlund, EPL **103**, 46003 (2013).
[4] L. Oddershede, P. Dimon, and J. Bohr, Phys. Rev. Lett. **71**, 3107–3110 (1993).
[5] T. D. de la Rubia, R. S. Averback, R. Benedek, and W. E. King, Phys. Rev. Lett. **59**, 1930–1933 (1987).
[6] D. J. Bacon and T. Diaz de la Rubia, J. Nucl. Mat. **216**, 275–290 (1994).
[7] K. Nordlund, M. Ghaly, R. S. Averback, M. Caturla, T. Diaz de la Rubia, and J. Tarus, Phys. Rev. B **57**, 7556–7570 (1998).
[8] K. Nordlund and R. S. Averback, Phys. Rev. B **59**, 20–23 (1999).
[9] A. F. Calder, D. J. Bacon, A. V. Barashev, and Y. N. Osetsky, Phil. Mag. **90**, 863 (2010).
[10] K. L. Merkle, *Radiation Damage in Metals*, edited by N. L. Peterson and S. D. Harkness (American Society for Metals, Metals Park, OH, 1976) p. 58.
[11] H. L. Heinisch, Rad. Eff. & Def. in Sol **113**, 53–73 (1990).
[12] E. Zarkadoula, M. T. Dove, K. Trachenko, S. L. Daraszewicz, D. M. Duffy, , M. Seaton, I. T. Todorov, and K. Nordlund, J. Phys. Condens. Matt. **25**, 125402 (2013).
[13] J. F. Ziegler, U. Littmark, and J. P. Biersack, *The stopping and range of ions in solids* (Pergamon New York, 1985) p. 321 p. :.
[14] C.-Y. Wei, M. I. Current, and D. N. Seidman, Phil. Mag. A **44**, 459–491 (1981), http://dx.doi.org/10.1080/01418618108239544.
[15] J. C. Moreno-Marin, U. Conrad, H. M. Urbassek, and A. Gras-Marti, Nucl. Instr. and Meth. B **48**, 404–407 (1990).
[16] P. R. Bevington, *Data reduction and error analysis for the physical sciences* (McGraw-Hill, New York, 1992).

[17]A. D. Backer, A. E. Sand, K. Nordlund, L. Luneville, D. Simeone, and S. L. Dudarev, *in preparation* (2016).
[18]M. T. Robinson and I. M. Torrens, Phys. Rev. B **9**, 5008 (1974).
[19]C.A.English and M. Jenkins, Materials Science Forum **15-18**, 1003–1022 (1987).
[20]N. Soneda, S. Ishino, and T. D. de la Rubia, Phil. Mag. Lett. **81**, 649–659 (2001),.
[21]K. Nordlund, J. Keinonen, M. Ghaly, and R. S. Averback, "Coherent displacement of atoms during ion irradiation," Nature **398**, 49–51 (1999).